

# Carbon Doping in $MgB_2$ : Role of Boron and Carbon $p_{x(y)}$ Bands

Prabhakar P. Singh

*Department of Physics, Indian Institute of Technology, Powai, Mumbai-400076, India*

---

## Abstract

We have studied the changes in the electronic structure and the superconducting transition temperature  $T_c$  of  $Mg(B_{1-x}C_x)_2$  alloys as a function of  $x$  with  $0 \leq x \leq 0.3$ . Our density-functional-based approach uses coherent-potential approximation to describe the effects of disorder, Gaspari-Gyorffy formalism to estimate the electron-phonon matrix elements and Allen-Dynes equation to calculate  $T_c$  in these alloys. We find that the changes in the electronic structure of  $Mg(B_{1-x}C_x)_2$  alloys, especially near the Fermi energy  $E_F$ , come mainly from the outward movement of  $E_F$  with increasing  $x$ , and the effects of disorder in the  $B$  plane are small. In particular, our results show a sharp decline in both  $B$  and  $C$   $p_{x(y)}$  states for  $0.2 \leq x \leq 0.3$ . Our calculated variation in  $T_c$  of  $Mg(B_{1-x}C_x)_2$  alloys is in qualitative agreement with the experiments.

*Key words:*

electronic structure, alloys, superconductivity

PACS: 74.25.Kc, 63.20.Kr

---

## 1 INTRODUCTION

The changes in the electronic properties of  $MgB_2$  upon doping with various elements gets manifested in the changes in its superconducting behavior. An understanding of these changes in the superconducting behavior of  $MgB_2$  upon doping can provide useful information about the nature of interaction responsible for superconductivity. Such information can then be used to prepare materials with desired superconducting properties. Since the discovery of superconductivity in  $MgB_2$ , a substantial amount of effort has been directed towards probing the various aspects of superconductivity using doping.

The effects of doping  $MgB_2$  with various elements such as  $s$ -elements  $Be$  [1] and  $Li$  [2],  $sp$ -elements  $Al$  [3,4] and  $Si$  [5], and  $d$ -elements  $Fe$ ,  $Co$ ,  $Ni$  [6] and others [7] have been studied experimentally. Most of these substitutions take place in the

$Mg$  plane of  $MgB_2$ , leaving the  $B$  plane in tact. For some dopants at particular concentrations, it is also found that the dopants prefer to form a separate layer [3,4] rather than mix with the  $Mg$  layer or the  $B$  layer. For dilute amount of dopants the changes in the superconducting properties, in particular the superconducting transition temperature,  $T_c$ , depends on the alloying element [1,2,3,4,5,6,7]. For larger concentrations, with only  $Mg_{1-x}Al_xB_2$  [3,4] being studied extensively, the  $T_c$  is found to decrease due to the gradual filling of the  $B$   $p_{x(y)}$ -holes.

The doping of  $MgB_2$  with  $C$  [8,9,10,11,12,13] can be expected to be different from the ones described in the previous paragraph due to the following two reasons, (i)  $C$  prefers to go to the  $B$  plane instead of the  $Mg$  plane and (ii)  $C$  forms strong covalent-bonded layered structure similar to  $B$  layer in  $MgB_2$ . These reasons imply that the lowering of  $T_c$  in  $Mg(B_{1-x}C_x)_2$  alloys with increasing  $x$  is mainly due to the filling up of the  $p_{x(y)}$  holes, and not due to disorder in the  $B$  plane. However, the  $x$  dependence of  $T_c$  in  $Mg(B_{1-x}C_x)_2$  alloys as obtained in some earlier experiments may not be accurate due to the difficulties in estimating its  $C$  content [13]. According to Ref. [13], the  $T_c$  observed for  $x = 0.1$  in  $Mg(B_{1-x}C_x)_2$  alloys was  $22 K$ , which is lower than the result of Ref. [12].

Theoretical attempts at understanding the changes in the electronic structure and how these changes affect the superconducting properties of carbon-doped  $MgB_2$  alloys have not gone beyond the rigid-band model approach [14] with its limited applicability. To be able to reliably describe the effects of  $C$  doping in  $MgB_2$ , we have carried out *ab initio* studies of  $Mg(B_{1-x}C_x)_2$  alloys with  $0 \leq x \leq 0.3$ . We have used Korringa-Kohn-Rostoker coherent-potential approximation [15,16] in the atomic-sphere approximation (KKR-ASA CPA) method for taking into account the effects of disorder, Gaspari-Gyorffy formalism [17] for calculating the electron-phonon coupling constant  $\lambda$ , and Allen-Dynes equation [18] for calculating  $T_c$  in  $Mg(B_{1-x}C_x)_2$  alloys as a function of  $C$  concentration. We have used the present approach to study several other  $MgB_2$ -based alloys [19,20,21]. In the following, we present our results in terms of the changes in the total density of states (DOS), in particular the changes in the  $p$  contributions of both  $B$  and  $C$  to the total DOS, as a function of concentration  $x$  of  $C$  atoms. Before we describe the results of our calculations we provide some of the computational details.

## 2 COMPUTATIONAL DETAILS

The charge self-consistent electronic structure of  $Mg(B_{1-x}C_x)_2$  alloys as a function of  $x$  has been calculated using the KKR-ASA CPA method [15,16]. We parametrized the exchange-correlation potential as suggested by Perdew-Wang [22] within the generalized gradient approximation [23]. The Brillouin zone (BZ) integration was carried out using 1215  $k$ - points in the irreducible part of the BZ. For DOS calculations, we added a small imaginary component of  $1 mRy$  to the energy and

used 4900  $\mathbf{k}$ -points in the irreducible part of the BZ. The lattice constants for  $Mg(B_{1-x}C_x)_2$  alloys as a function of  $x$  were taken from the experimental result of . The Wigner-Seitz radius for  $Mg$  was larger than that of  $B$  and  $C$ . The sphere overlap which is crucial in ASA, was less than 10% and the maximum  $l$  used was  $l_{max} = 2$ . The present calculations were carried out using the scalar-relativistic Schrodinger equation. The Green's function is calculated in a complex plane with a 20 point Gaussian quadrature.

The electron-phonon coupling constant  $\lambda$  was calculated using Gaspari-Gyorffy [17] formalism with the charge self-consistent potentials of  $Mg(B_{1-x}C_x)_2$  obtained with the KKR-ASA CPA method. Subsequently, the variation of  $T_c$  as a function of  $C$  concentration was calculated using Allen-Dynes equation [18]. The parameters used in the calculation of  $T_c$  using the Allen-Dynes equation, for the whole range of  $x$ , were  $\mu^* = 0.09$ ,  $\omega_{rms} = 400 \text{ cm}^{-1}$ , and  $\omega_{ln} = 834 \text{ K}$ .

### 3 RESULTS AND DISCUSSION

In this section we describe our results for  $Mg(B_{1-x}C_x)_2$  alloys in terms of the changes in the densities of states, the electron-phonon coupling constant  $\lambda$  and the superconducting transition temperature  $T_c$  as a function of  $x$  with  $0 \leq x \leq 0.3$ . In our analysis we will emphasize those aspects of changes in the electronic structure which directly affect the superconducting properties of  $Mg(B_{1-x}C_x)_2$  alloys, in particular its  $T_c$ . Thus, we discuss the changes in the density of states as a function of  $x$ , in particular the  $p$  contributions of both  $B$  and  $C$  to the total DOS and how it affects the electron-phonon coupling constant and consequently the  $T_c$  of  $Mg(B_{1-x}C_x)_2$  alloys.

#### 3.1 Densities of States

In Fig. 1, we show the total DOS of  $Mg(B_{1-x}C_x)_2$  alloys for  $x$  equal to 0.01, 0.1, 0.2 and 0.3, calculated using the KKR-ASA CPA method. A comparison of Figs. 1(a)-(d) shows that with increasing  $x$  the Fermi energy,  $E_F$ , moves outward and the DOS becomes smoother. The outward movement of  $E_F$  is due to the increase in the number of valence electrons with the addition of  $C$  while the increase in disorder in the  $B$  plane of  $MgB_2$  flattens the peaks in the DOS. In  $Mg(B_{1-x}C_x)_2$  alloys the outward movement of  $E_F$  decreases the total DOS at the Fermi energy,  $N(E_F)$ , in particular for  $x \sim 0.3$ ,  $N(E_F)$  is a minimum. Generally, a decrease in  $N(E_F)$  leads to a lowering of  $T_c$ , it is expected that with the increase in  $C$  concentration the  $T_c$  of  $Mg(B_{1-x}C_x)_2$  alloys should decrease.

It is known that in  $MgB_2$  the holes in the  $p_{x(y)}$  bands couple very strongly to the

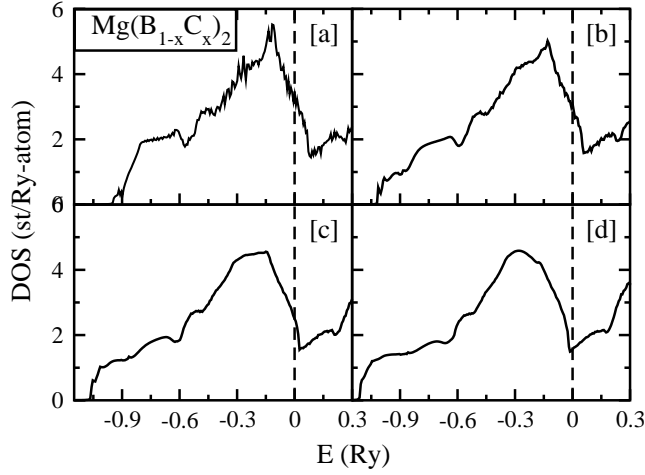


Figure 1. The calculated total density of states (solid line) of  $Mg(B_{1-x}C_x)_2$  alloys for (a)  $x = 0.01$ , (b)  $x = 0.1$ , (c)  $x = 0.2$  and (d)  $x = 0.3$ , respectively. The dashed vertical line indicates the Fermi energy.

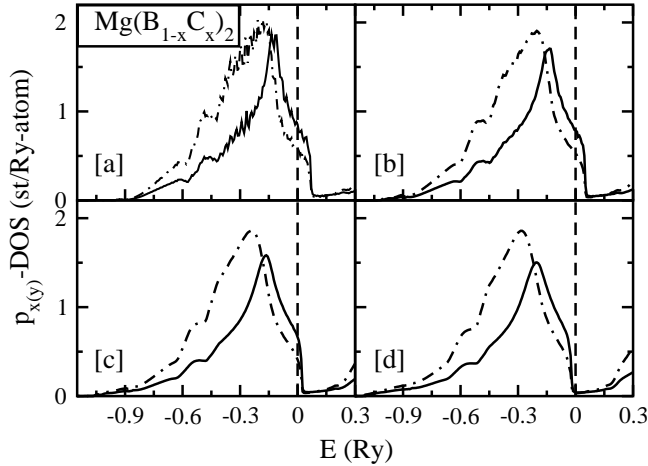


Figure 2. The calculated  $p_{x(y)}$  density of states for both  $B$  (solid line) and  $C$  (dot-dashed line) in  $Mg(B_{1-x}C_x)_2$  alloys at (a)  $x = 0.01$ , (b)  $x = 0.1$ , (c)  $x = 0.2$  and (d)  $x = 0.3$ , respectively. The dashed vertical line indicates the Fermi energy.

optical  $E_{2g}$  phonon mode [24,25,26,27], and hence a change in the  $p_{x(y)}$  bands directly affects the superconducting properties of  $MgB_2$ . Thus, to get a more detailed picture of how the changes in  $N(E_F)$  affect the superconducting properties of  $MgB_2$ , we have to analyze the changes in the  $B$   $p_{x(y)}$  contributions to  $N(E_F)$ . In addition, since  $C$  is known to form strong covalent-bonded layered structures, it may be that in  $Mg(B_{1-x}C_x)_2$  alloys the  $C$   $p_{x(y)}$  electrons/holes also couple to the optical phonons the way  $B$   $p_{x(y)}$  electrons/holes do.

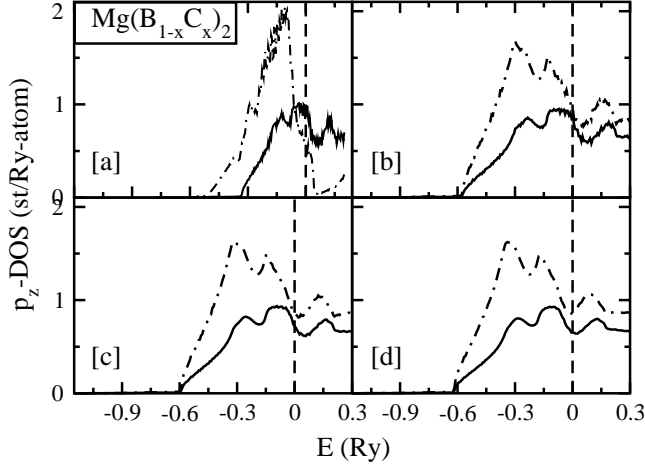


Figure 3. The calculated  $p_z$  density of states for both  $B$  (solid line) and  $C$  (dot-dashed line) in  $Mg(B_{1-x}C_x)_2$  alloys at (a)  $x = 0.01$ , (b)  $x = 0.1$ , (c)  $x = 0.2$  and (d)  $x = 0.3$ , respectively. The dashed vertical line indicates the Fermi energy.

To see how the  $p$  contributions to the total DOS change in  $Mg(B_{1-x}C_x)_2$  alloys as a function of  $x$ , we show in Fig. 2 the  $p_{x(y)}$  DOS for both  $B$  and  $C$  in  $Mg(B_{1-x}C_x)_2$  alloys for  $x$  equal to 0.01, 0.1, 0.2 and 0.3. The  $p$  DOS of  $MgB_2$  calculated with the KKR-ASA CPA method is in good agreement with our full-potential result [28] and other calculations [29,30], indicating the reliability of the present approach. From Fig. 2 it is clear that near  $E_F$  both  $B$  and  $C$   $p_{x(y)}$  densities of states are similar for the whole range of  $x$  with  $C$  DOS being somewhat smaller than the  $B$  DOS. As the addition of  $C$  increases the electron count, the outward movement of  $E_F$  as  $x$  increases fills up the  $p_{x(y)}$  bands of both  $B$  and  $C$ , signalling a sharp change in the superconducting properties of  $Mg(B_{1-x}C_x)_2$  alloys in this range.

The changes in the  $p_z$  contribution to the total DOS in  $Mg(B_{1-x}C_x)_2$  alloys as a function of  $x$  is not very significant, as can be seen from Fig. 3, where we have shown the  $p_z$  DOS for both  $B$  and  $C$  in  $Mg(B_{1-x}C_x)_2$  alloys for  $x$  equal to 0.01, 0.1, 0.2 and 0.3. In the dilute limit, the  $p_z$  DOS due to  $B$  in  $Mg(B_{1-x}C_x)_2$  alloy is similar to the  $p_z$  DOS due to  $B$  in  $MgB_2$  [28,30,31]. In addition, these electrons play a minor role in deciding the superconducting properties of  $Mg(B_{1-x}C_x)_2$  alloys.

Since the changes in the superconducting properties of  $Mg(B_{1-x}C_x)_2$  are dictated by the DOS at  $E_F$ , in particular the  $p_{x(y)}$  contributions of both  $B$  and  $C$  to the total DOS, we show in Fig. 4 the variations of the total density of states  $N(E_F)$  and the  $B$  and  $C$   $p_{x(y)}$  contributions to it. As can be seen from Fig. 4, there is a steep drop in the  $p_{x(y)}$  DOS for both  $B$  and  $C$  between  $x = 0.2$  to  $x = 0.3$ , indicating the filling up of the  $p_{x(y)}$  bands. Given that the  $p_{x(y)}$  bands are responsible for driving superconductivity in  $MgB_2$ , we expect the superconducting properties of  $Mg(B_{1-x}C_x)_2$  alloys to change significantly between  $x = 0.2$  to  $x = 0.3$ .

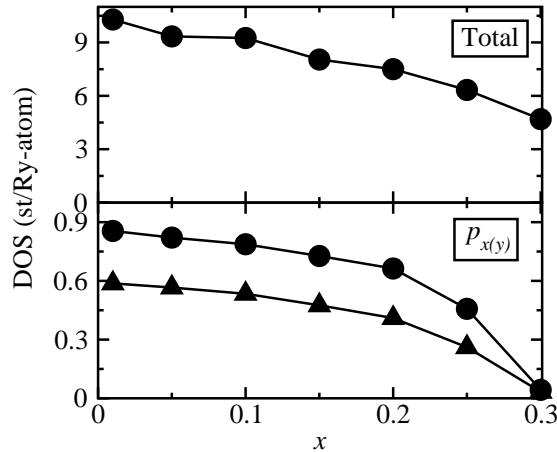


Figure 4. The calculated variation in the total (upper panel) and the  $p_{x(y)}$  (lower panel) densities of states at the Fermi energy as a function of  $x$  in  $Mg(B_{1-x}C_x)_2$  alloys. In the lower panel, both  $B$  (filled circle) and  $C$  (filled triangle)  $p_{x(y)}$  densities of states are shown.

Here, we like to point out that the range of  $x$  as indicated above, in which the superconducting properties of  $Mg(B_{1-x}C_x)_2$  are expected to change significantly, must be viewed within the constraints inherent in the present approach.

### 3.2 The superconducting transition temperature

We have used the Gaspari-Gyorffy formalism to calculate the Hopfield parameter and then the electron-phonon coupling constant  $\lambda$  of  $Mg(B_{1-x}C_x)_2$  alloys. Our calculations show that the  $C$  atoms in  $Mg(B_{1-x}C_x)_2$  alloys couple to the phonons as strongly as the  $B$  atoms. For example, at  $x = 0.2$  we find  $\lambda$  (per atom) for  $B$  and  $C$  to be 0.31 and 0.24, respectively. It is interesting to note that as the  $C$   $p_{x(y)}$  bands fill up somewhat later than the  $B$   $p_{x(y)}$  bands, the calculated  $\lambda$  of  $C$  becomes greater than that of  $B$  for  $x \sim 0.3$ .

To see how the changes in the electronic properties of  $Mg(B_{1-x}C_x)_2$  alloys affect the superconducting transition temperature, we show in Fig. 5 the calculated  $T_c$  as a function of  $x$  in  $Mg(B_{1-x}C_x)_2$  alloys. The experimentally observed  $T_c$  values as reported in Refs. [12,13] are also shown in Fig. 5. Note that for  $x = 0.1$ , Refs. [12] and [13] find  $T_c$  to be equal to 34 K and 22 K, respectively. Our calculations show that the  $T_c$  drops to  $\sim 0$  K from 20 K as  $x$  changes from 0.2 to 0.3, which is consistent with the filling up of the  $p_{x(y)}$  bands as discussed above. The calculated trend in the variation of  $T_c$  in  $Mg(B_{1-x}C_x)_2$  alloys is in qualitative agreement with the experimental results as shown in Fig. 5.

Some of the differences between the calculated (more accurately than the present

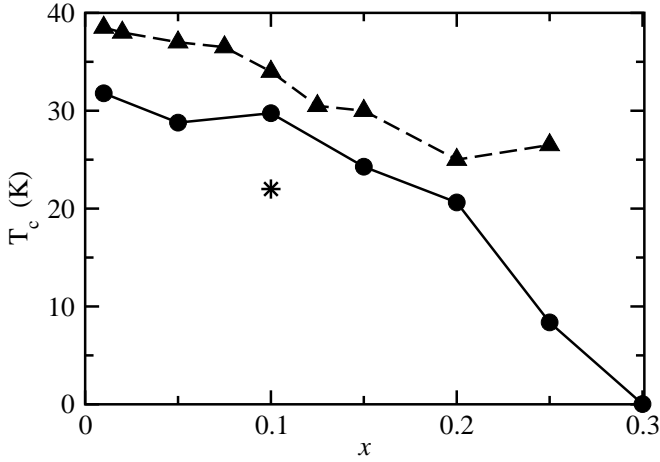


Figure 5. The calculated (filled circle) variation of  $T_c$  as a function of concentration  $x$  in  $Mg(B_{1-x}C_x)_2$  alloys. The experimental results of Ref. [12] (filled triangle) and Ref. [13] (star) are also shown.

approach) and the observed  $T_c$  in  $Mg(B_{1-x}C_x)_2$  alloys may be due to an inaccurate determination of the  $C$  content in these alloys, as pointed out in Ref. [13]. In the present case, the calculation of  $T_c$  incorporates two additional approximations, (i) use of a constant phonon frequency over the whole range of  $x$  and (ii) use of Gaspari-Gyorffy formalism for estimating the electron-phonon matrix elements, which is known to underestimate the strength of the coupling. However, we expect the trend in the variation of  $T_c$  in  $Mg(B_{1-x}C_x)_2$  alloys, as shown in Fig. 5, to be reliable.

## 4 CONCLUSIONS

We have studied the changes in the electronic structure of  $Mg(B_{1-x}C_x)_2$  alloys as a function of  $x$  with  $0 \leq x \leq 0.3$  using the KKR-ASA CPA method. We find that the changes in the electronic structure of  $Mg(B_{1-x}C_x)_2$  alloys, especially near the Fermi energy  $E_F$ , come mainly from the outward movement of  $E_F$  with increasing  $x$  and the effects of disorder in the  $B$  plane are small. In particular, our results show a sharp decline in  $B$  and  $C$   $p_{x(y)}$  states for  $0.2 \leq x \leq 0.3$ . Our calculated variation in  $T_c$  of  $Mg(B_{1-x}C_x)_2$  alloys is in qualitative agreement with the experiments.

## References

- [1] I. Felner, Physica C 353 (2001) 11.

- [2] Y. G. Zhao, X. P. Zhang, P. T. Qiao, H. T. Zhang, S. L. Jia, B. S. Cao, M. H. Zhu, Z. H. Han, X. L. Wang, B. L. Gu, *Physica C* 361 (2001) 91.
- [3] J. Y. Xiang, D. N. Zheng, J. Q. Li, L. Li, P. L. Lang, H. Chen, C. Dong, G. C. Che, Z. A. Ren, H. H. Qi, H. Y. Tian, Y. M. Ni, Z. X. Zhao, cond-mat/0104366.
- [4] J. S. Slusky, N. Rogado, K. A. Regan, M. A. Hayward, P. Khalifah, T. He, K. Inumaru, S. M. Loureiro, M. K. Haas, H. W. Zandbergen, R. J. Cava, *Nature* 410 (2001) 343.
- [5] M. R. Cimberle, M. Novak, P. Manfrinetti, A. Palenzona, cond-mat/0105212.
- [6] Y. Moritomo, S. Xu, cond-mat/0104568.
- [7] C. Buzea, T. Yamashita, *Superconductors, Science and Technology* 14 (2001) R115.
- [8] J. S. Ahn, E. J. Choi, cond-mat/0103069.
- [9] M. Paranthaman, J. F. Thompson, D. K. Christen, *Physica C* 355 (2001) 1.
- [10] T. Takenobu, T. Ito, D. H. Chi, K. Prassides, Y. Iwasa, *Phys. Rev. B* 64 (2001) 134513.
- [11] S. Zhang, J. Zhang, T. Zhao, C. Rong, B. Shen, Z. Cheng, cond-mat/0103203.
- [12] A. Bharathi, S. J. Balaselvi, S. Kalavathi, G. L. N. Reddy, V. S. Sastry, Y. Haritharan, T. S. Radhakrishnan, *Physica C* 370 (2002) 211.
- [13] R. A. Ribeiro, S. Bud'ko, C. Petrovic, P. C. Canfield, *Physica C* 382 (2002) 166.
- [14] M. J. Mehl, D. A. Papaconstantopoulos, D. J. Singh, *Phys. Rev. B* 64 (2001) 134513.
- [15] P. P. Singh, A. Gonis, *Phys. Rev. B* 49 (1994) 1642.
- [16] J. Faulkner, *Prog. Mat. Sci.* 27 (1982) 1.
- [17] G. Gaspari, B. L. Gyorffy, *Phys. Rev. Lett.* 28 (1972) 801.
- [18] P. B. Allen, R. C. Dynes, *Phys. Rev. B* 12 (1975) 905.
- [19] P. J. T. Joseph, P. P. Singh, *Solid State Commun.* 121 (2002) 467.
- [20] P. P. Singh, *Physica C* 382 (2002) 381.
- [21] P. P. Singh, P. J. T. Joseph, *J. Phys.:Condens. Matter* 14 (2001) 12441.
- [22] J. P. Perdew, Y. Wang, *Phys. Rev. B* 45 (1992) 13244.
- [23] J. P. Perdew, K. Burke, M. Ernzerhof, *Phys. Rev. Lett.* 77 (1996) 3865.
- [24] Y. Kong, O. V. Dolgov, O. Jepsen, O. K. Andersen, *Phys. Rev. B* 64 (2001) 20501.
- [25] K.-P. Bohnen, R. Heid, B. Renker, *Phys. Rev. Lett.* 86 (2001) 5771.
- [26] H. J. Choi, D. Roundy, H. Sun, M. L. Cohen, S. G. Louie, *Phys. Rev. B* 66 (2002) 020513.
- [27] P. P. Singh, *Solid State Commun.* 125 (2003) 323.



- [28] P. P. Singh, Phys. Rev. Lett. 87 (2001) 087004.
- [29] J. Kortus, I. I. Mazin, K. D. Belashchenko, V. P. Antropov, L. L. Boyer, Phys. Rev. Lett. 86 (2001) 4656.
- [30] Y. Zhu, A. R. Moodenbaugh, G. Schneider, J. W. Davenport, T. Vogt, Q. Li, G. Gu, D. A. Fischer, J. Tafto, Phys. Rev. Lett. 88 (2002) 247002.
- [31] R. F. Klie, Y. Zhu, G. Schneider, J. Tafto, cond-mat/0301575.